

# Canterbury Drifts at Ocean Drilling Program Site 1119, New Zealand: Climatic modulation of southwest Pacific intermediate water flows since 3.9 Ma

R.M. Carter\* Marine Geophysical Laboratory, James Cook University, Townsville, QLD 4811, Australia

C.S. Fulthorpe

H. Lu

} Institute for Geophysics, University of Texas, Austin, Texas 78712, USA

## ABSTRACT

We provide a record of variations in southwest Pacific Ocean intermediate water flow that shows a strong correlation between periods of vigorous flow and warm climate phases. Ocean Drilling Program Site 1119, located at 395 m water depth on the upper continental slope east of New Zealand, penetrated 514 m of silts and silty clays (glacial deposits) punctuated by muds and episodic 0.02–1.2-m-thick terrigenous sands (interglacial deposits). The natural gamma-ray record reflects the waxing and waning of the South Island ice cap since 3.91 Ma. Below 86.19 m composite depth, the succession comprises drift sediments deposited from north-flowing intermediate Subantarctic Mode Water (SAMW, ~250–800 m depth) and Antarctic Intermediate Water (~800–1100 m depth). A change from the deposition of large, low-energy drifts on the middle slope to smaller, higher-energy drifts on the upper slope coincided with global climatic deterioration that occurred after ca. 3.25 Ma. This change marks an upward expansion of intermediate cold waters, perhaps caused by the inception of the Subantarctic Front and the consequent commencement of Southland Current-driven SAMW flow.

**Keywords:** Ocean Drilling Program, Antarctic Intermediate Water, Subantarctic Mode Water, Subantarctic Front, Canterbury Drifts, sediment drifts, New Zealand.

## INTRODUCTION

Ocean Drilling Program Site 1119 was located to provide information about Southern Hemisphere midlatitude climate change (history of the Southern Alps ice cap; Carter and Gammon, 2004), oceanic Subtropical Front (STF) and Subtropical Water–Subantarctic Water (SAW) mass migrations (Carter et al., 2004b), and the relationships between sediment-drift deposition, climate cycling, and intermediate-depth water flows. These three latter relationships are the subject of this paper.

Site 1119 is located 100 km offshore from eastern South Island, New Zealand, in a water depth of 395 m, just oceanward of the shelf edge (~150 m depth) and on the SAW side of the STF (Fig. 1, inset). Sediment is shed eastward from the Southern Alps (Mount Cook, 3754 m), which are along the Alpine fault plate boundary between the Pacific and Australian plates, into about eight major river systems, three of which coalesce to form the 250-km-long braidplain of the Canterbury Plains and deliver ~15 Mt of sediment annually to the east coast shoreline (Griffiths and Glasby, 1985; Hicks and Shankar, 2003). During recent sea-level lowstands, the Canterbury Plains extended as much as 150 km from the mountain front toward Site 1119, which was

then located within ~30 km of the glacial shoreline and subject to the direct influence of glacial-riverine sediment plumes.

Seaward of the STF, SAW circulates north and clockwise in a cold-water gyre within the head of the Bounty Trough. Beneath this surface-water mass, cold, intermediate-depth waters also travel northward along the eastern New Zealand margin (Morris et al., 2001). Subantarctic Mode Water (SAMW), formed by seasonal convection at the Subantarctic Front (SAF) (McCartney, 1982), is present at depths of ~250–800 m, entrained within the Southland Current (Sutton, 2003), and Antarctic Intermediate Water (AAIW), derived by subduction at the Antarctic Front, is between ~800 and 1100 m (Lynch-Stieglitz et al., 1994).

## STRATIGRAPHIC SETTING

The South Island shelf is underlain by eastward-prograding clinoforms of the lower Miocene to Holocene Otakou Group (Carter and Carter, 1982) (Fig. 1). Sediment has been shed from the mountainous western South Island since the inception of the Pacific–Australia plate boundary there in the latest Oligocene to early Miocene (Wellman, 1971; Norris and Carter, 1982; Carter et al., 2004a). The inner edge of the shelf-sediment prism is exposed on land, where mildly uplifted Bluecliffs

Formation—the onshore equivalent of the Site 1119 sediments—comprises gray terrigenous siltstone with archibenthal molluscan and microfossil faunas (Morgans et al., 1999). This siltstone shoals upward gradationally into shallow-marine sands with shoreface molluscan faunas (Southburn Sand; Gair, 1959) and thereafter into nonmarine coastal-plain sediment (Carter, 1988) and piedmont gravel (Browne and Naish, 2003). A similar stratigraphy, without the coastal-plain sediment cap, is present in all offshore petroleum exploration holes through the shelf prism (e.g., *Clipper-1*; British Petroleum et al., 1984). The eastern South Island shelf varies in width from 37 to 122 km, implying average progradation rates of 1.5–1.9 km/m.y. since the shelf started building eastward in the late Oligocene. Typical linear sedimentation rates for the Bluecliffs Formation are 5 cm/k.y. at the type locality (Morgans et al., 1999) and as high as 15 cm/k.y. at offshore exploration wells (Carter, 1988).

Clinof orm shelf-slope geometry and associated continental-slope mud successions are generally interpreted as evidence for the bypassing of sediment across the shelf into deeper-water, lower energy depositional locations by “mud hopping” or “turbid-layer bypass” (Cotton, 1918; Stanley, 1985). However, this process alone cannot explain the well-developed sediment drifts that occur on many seismic profiles through the Canterbury prograding shelf-slope complex (Fulthorpe and Carter, 1991; Lu et al., 2003; Lu and Fulthorpe, 2004). The largest drifts are as large as 55 km long, 20 km wide, and 1 km thick. Smaller drifts, termed “sediment waves” by Lu and Fulthorpe (2004), are mostly no bigger than 10 km long, 3 km wide, and 0.1 km thick. Long axes of drifts are aligned as much as 15° more westward than the northeastward strike of the local slope. Individual drifts migrated westward (upslope) under the influence of the Coriolis effect, and the locus of drift deposition migrated northward consistent with the direction of intermediate-depth water movement. At any time, the active drifts were concentrated along the midslope, seaward of the contemporary shelf edge from which they were separated by a channel-like gutter. After

\*E-mail: bob.carter@jcu.edu.au.

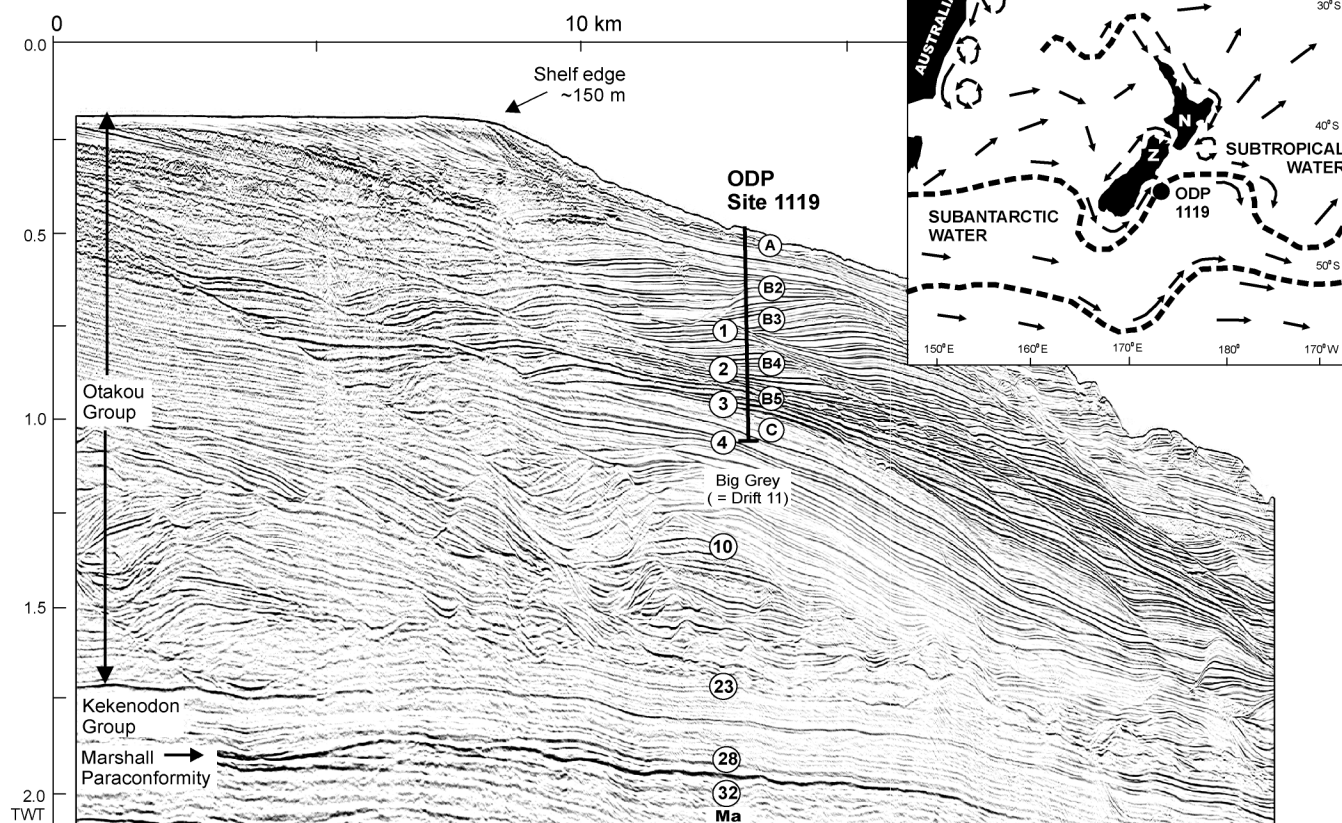


**Figure 1.** High-resolution multichannel seismic profile (R/V *Maurice Ewing* cruise EW00-01; Lu and Fulthorpe, 2004) across eastern New Zealand margin, through Ocean Drilling Program (ODP) Site 1119. Inset is location map. Three distinctive stratigraphic intervals were penetrated by drilling: A—upper-slope clinoforms, which represent progradation of shore-connected deltaic foresets during glacial lowstands, with intercalated interglacial sand-mud drapes; B—small midslope sediment drifts, deposited obliquely along slope (upslope climbing) from northward-traveling Subantarctic Mode Water (SAMW); and C—large lower-midslope sediment drifts of similar architecture to B, but inferred to be migrating less rapidly. Circled numbers to left of drill site indicate approximate age (in Ma). Detailed characteristics of units A–C are presented in Figure 2 (see text footnote 1), where marked reflectors 11–19 correspond to junctions between individual foreset sets or drifts and seismic mapping horizons of Lu and Fulthorpe (2004).

attaining their maximum size, individual drifts become welded to the shelf edge by infill of the gutter on their upslope side.

## SEDIMENT LITHOLOGY

Site 1119 (Fig. 2<sup>1</sup>) penetrated 86.19 m of upper-slope terrigenous silt and fine sand (unit A; 0–0.252 Ma; marine oxygen isotope stages [MIS] 1–7), which are underlain across a 25 k.y. unconformity by 428 m of similar late Pliocene–Pleistocene sediment (units B–C; 0.28–3.92 Ma; MIS 8–Gi-11) (Carter et al., 2004b). Unit A (MIS 1–7) sediments above the unconformity represent the last two glacial-interglacial cycles. They comprise downlapping shelf-edge clinoforms deposited on the upper slope, ~5 km seaward of the shelf break and ~30 km seaward of the MIS 2 lowstand shoreline. Unit B contains a higher ratio of sand and corresponds to the deposition of approximately seven small midslope sediment

drifts. Unit C is massive silt and clayey silt, lacks sand, and corresponds to the upper part of a single large sediment drift. The disposition of these units, the amount of sand that they contain, and their sedimentation rates are summarized in Figure 2 (see footnote 1). Overall, Site 1119 records a sand thickness of 53.82 m out of a total sediment thickness of 513.5 m, i.e., an average sand:mud ratio of 1:9.5, and represents a shoaling-upward succession from ~900 to ~400 m water depth.

Site 1119 cores and formation micro-scanner (FMS) images show that units B and C, below 86.19 m composite depth (mcd), comprise centimeter-scale-bedded silt, clayey silt, and silty clay, variously burrowed or bioturbated, and punctuated by 0.2–1.5-m-thick beds of fine-grained quartzofeldspathic sand (mean size, 130  $\mu$ m) and muddy sand. Internally, the thicker sand units often display pulsatory changes in sand or silt content; organized Bouma turbidite structures (e.g., Stow et al., 1998) are generally not present. Some sands have both gradational bottoms and tops and

comprise a reverse- to normal-graded mud-sand-mud triplet, similar to other described sediment-drift deposits and to the idealized drift facies models of Faugeres et al. (1984) and Stow et al. (1998). The overall characteristics of the Site 1119 muds and sands below 86.19 mcd coincide with those first described for sediment drifts from the Feni Drift, viz., “contacts between the different facies may be more or less planar and sharp, distinctly erosional, or completely gradational, and all three types are equally common at the base or at the top of separate beds. . . . Mottling occurs throughout. . . . together with other more or less distinct and isolated pockets and streaks. . . . Bioturbation was clearly a continuous process that has modified or destroyed much of the original nature of the contacts” (Faugeres et al., 1984, p. 298). Virtually all of the cored sediments of the Canterbury Drift, between 86.19 and 514 mcd (total depth at Site 1119), therefore, belong to the silt and sand, mottled silt and mud, and homogeneous mud sediment-drift facies of Faugeres et al. (1984) and Stow et al. (1998).

<sup>1</sup>Loose insert: Figure 2. Lithology and physical properties for Site 1119 plotted against geomagnetic polarity scale (GPS).



Together with the complete double-graded drift motif, “top-only” and “mid-only” motif varieties (Stoker et al., 1998) are common in the Canterbury Drifts, though without the macroscopic millimeter-scale lamination and wispy lamination described from some other drift deposits. Nonetheless, the presence of pervasive centimeter-scale bedding in the background silty clay and clayey silt of units B and C, together with their large-scale seismic geometry (Fig. 1), indicate deposition from gentle, rhythmically fluctuating bottom currents. The fine-silt grain-size mode varies between  $\sim 12$  and  $25\ \mu\text{m}$ . Comparison with sortable silts described from other (but abyssal) sediment drifts suggests deposition from currents with mean speeds of  $\sim 5$ – $15\ \text{cm/s}$  (e.g., McCave et al., 1996). These speeds correspond to the mid-range of velocities measured within the modern Southland Current in eastern New Zealand (Sutton, 2003). Against this background, the sands that occur interspersed throughout the unit B drifts are interpreted to have been emplaced during periods of enhanced bottom-current activity. The common presence of sharp bases to the interglacial sand beds, in particular, indicates that the emplacing currents were strong enough to cause seabed erosion of clayey silt. Typical sand-bed grain sizes are  $\sim 120$ – $250\ \mu\text{m}$ , indicating that the depositional currents attained speeds of  $20$ – $30\ \text{cm/s}$  or more at  $1\ \text{m}$  above the bed (Miller et al., 1977). The common occurrence of normally graded, muddy tops to sand beds indicates that a gradual waning of current speed occurred. The  $328\ \text{m}$  thickness of units B and C only contains two thin ( $<1\ \text{cm}$  thick) beds of graded sand that might be interpreted as slope turbidites (Carter et al., 1999).

## DISCUSSION

Site 1119 shows well the effect of glacial-interglacial climatic fluctuations on sedimentary processes in a zone of intermediate-depth current drifts on the middle to upper continental slope. Small current drifts similar to those of unit B occur at the modern seafloor at slope depths of  $1100\ \text{m}$ , downslope from Site 1119. That the small upper-slope drifts of unit B do not extend to the seabed at Site 1119 may result from a combination of shelf-edge subsidence and an increased magnitude of glacial-interglacial cycling through the late Pleistocene, which caused successive low-stand shorelines to deliver their terrigenous load in increasing proximity to the shelf edge. Hinterland uplift, and hence increased sediment supply into upper-slope clinoforms, may also have played a role (Lu and Fulthorpe, 2004).

The unit B drift interval was deposited on the upper slope  $\sim 30\ \text{km}$  seaward of the shelf

edge and in inferred paleo-water depths of  $400$ – $800\ \text{m}$ . Individual drifts are well delineated by spaced, strong, and continuous sigmoidal reflectors (Fig. 1). The main bodies of three small drifts, B2–B4, were intersected by the drill hole. Thin interval B1, comprising MIS 9, displays seismic characteristics intermediate between those of unit A and underlying units B2–B4; this interval has been included within unit B because of its location beneath the downlap unconformity at the base of unit A. The boundaries between individual drifts B2–B4, and other nearby drifts visible on the seismic records, exhibit evidence of local erosion, but the essentially complete nature of the Site 1119 climatic record (Fig. 2; cf. Carter and Gammon, 2004) suggests that little sediment is missing, even at the boundaries between major drifts.

Drifts B1–B4 are underlain by a seismic interval within which the reflections are stronger, more closely spaced than above, and slightly irregular (Fig. 1). Landward, these reflectors pass laterally into small slope drifts similar to (but older than) drifts B2–B4, and we therefore interpret this interval, B5, as the seaward tail of these upslope drifts. B5 corresponds with the presence in the drill core of an interval of graded calcareous sands within a background of silty clays and silts similar to those in drifts B2–B4 (Fig. 2). The condensed nature of the B5 drift tails is indicated by the common presence in B5 sands of glauconite and carbonate contents of  $>50\%$ , shell fragments, and abundant calcareous plankton.

The base of unit B5 at  $445\ \text{mcd}$  is marked by the deepest calcareous sand bed and a sharp stratigraphic change (Fig. 2). Beneath B5, the sediments comprise homogeneous silty clays, clayey silts, and silts of uniformly low sand and carbonate content (unit C1), which pass into slightly calcareous silty clay at the base of the hole (C2). Seismically, units C1 and C2 comprise the upper part of the large midslope drift termed Big Grey (Carter et al., 1999). This drift was deposited on the middle slope in estimated paleo-water depths of  $\sim 800$ – $1400\ \text{m}$ , and Lu et al. (2003; their Drift 11) estimated that it commenced growth in the early-late Miocene, ca.  $10.5\ \text{Ma}$ .

The change in drift style that occurred at  $3.25\ \text{Ma}$  was accompanied by the incoming of pulsed carbonate-rich sands (Fig. 2). Though active tectonism was occurring in the South Island hinterland from the Miocene onward (e.g., Carter et al., 2004a), tectonic events are unlikely to have been the primary control on this dramatic facies change. Rather, the change represents an increase in seabed hydraulic energy together with an increase in production of both seafloor and planktonic calcareous fauna; i.e., the  $3.25\ \text{Ma}$  change resulted from oceanographic rather than orogenic causes.

## INTERPRETATION

The results from Site 1119 confirm the expectation that Canterbury sediment-drift deposition occurred in concert with fluctuations in the northward flow of Southland Current-driven SAMW and perhaps also in the deeper AAIW water mass (cf. Lynch-Stieglitz et al., 1994; Morris et al., 2001; Sutton, 2003). The site provides a detailed record of the relationship between intermediate-depth water flow, drift sedimentation, and climate change at several different time scales.

First, at the scale of individual glacial-interglacial cycles, there is a close correlation between the deposition of the thicker (and coarser grained) sand beds, which signal enhanced bottom-current speeds, and the occurrence of periods of warmer climate (Fig. 2). Some, mostly thin, sand beds also occur in cold climatic intervals at Site 1119 and perhaps especially within the transition zone between cold and warm periods. These patterns are consistent with the reports by Stow et al. (1986) and McCave et al. (1995) of enhanced current flows of intermediate-depth water during interglacial periods in the North Atlantic and with the enhanced thermohaline circulation inferred by Stow et al. (1986), Duplessy et al. (1991), and Groger et al. (2003) to occur at glacial-interglacial transitions. One result of warming conditions, therefore, may be the enhanced production around Antarctica of cold surface meltwater that then sinks at cold-water fronts to form vigorous AAIW and SAMW flows. Whatever the precise mechanism, however, a link between warm climate and more vigorous advection of Pacific Ocean intermediate-water flows extends back at least to  $3.25\ \text{Ma}$  in the late Pliocene (Fig. 2).

Second, over longer time scales, a relationship exists between the stratigraphy and sedimentology of the Canterbury Drifts and the late Cenozoic global climate deterioration. Marine oxygen isotope records indicate that late Cenozoic climatic cooling occurred mostly in two phases, a two-step decline between  $16$  and  $10\ \text{Ma}$  (enhancement of the East Antarctic Ice Sheet; Cooper and O'Brien, 2004) and a final deterioration between  $3$  and  $0\ \text{Ma}$  (formation of the boreal ice sheets) (e.g., Zachos et al., 2001). The small elongate drifts D1–D8 that underlie the Big Grey drift (D11) (Fig. 1) were initiated ca.  $15\ \text{Ma}$  (Lu and Fulthorpe, 2004). Their commencement may represent the inception of the Antarctic Front and AAIW flows, in parallel with the observed  $16$ – $10\ \text{Ma}$  global cooling. The late Miocene to early Pliocene ( $10$ – $3\ \text{Ma}$ ), a period of less variable climate prior to resumed post- $3\ \text{Ma}$  cooling, coincided with the deposition of the Big Grey mud drift, consistent with lower-velocity intermediate-depth flows at the time.

At 3.25 Ma (MIS 138), deposition of Drift A (Big Grey) ceased, to be replaced by the B sequence of small upper-slope drifts centered ~20 km farther west (Fig. 2). The tails of these drifts extend seaward across Site 1119 as interval B5. The upslope migration of drift deposition into shallower waters was thus accompanied by a diminution of drift size and, concomitantly, by the increase in grain size and current velocity marked by the appearance of carbonate-rich sand beds in B5. This major environmental change was followed, after further global cooling, by the initiation of drift B4 at 1.95 Ma (MIS 73). The change from a large, low-energy (mud) drift to smaller, shallower-water and higher-energy (sandy) drifts was therefore accompanied first, by the commencement of global late Pliocene–Pleistocene cooling and second, by an increased amplitude of climatic fluctuation from MIS 100 onward. These changes may have resulted successively from (1) the 3.25 Ma start of new, shallower, and more vigorous intermediate-depth water flow (SAMW), perhaps caused by the initiation of the SAF and subsequent appearance of the Southland Current seaward of an intensified STF, and (2) the post-2.5 Ma downslope expansion of SAMW flows driven by the more intensive glaciations that occurred from MIS 100 onward.

# ACKNOWLEDGMENTS

We thank Dietz Warnke and Pat De Deckker for their careful critical reading of the manuscript. Carter thanks the members of the scientific and technical parties and the crew of R/V *JOIDES Resolution* for the contributions they made toward the collection, logging, and shipboard interpretation of Site 1119 cores on Leg 181. Fulthorpe thanks J.A. Austin, G. Browne, R. Burger, D. Cathro, J. Diebold, S. Herr, S. Sastrup, and the crew of R/V *Maurice Ewing* for their assistance in collecting seismic data on cruise EW00-01. This research used samples and data provided by the Ocean Drilling Program, sponsored by the U.S. National Science Foundation (NSF) and participating countries under management of Joint Oceanographic Institutions (JOI), Inc. Financial support has been provided by NSF grants OCE-97313031 and OCE-0221182 to Fulthorpe and Australian Research Council grant A-39805139 to Carter.

# REFERENCES CITED

British Petroleum, Shell, and Todd, 1984, Drilling completion report *Clipper-1*, PPL 38202, offshore Canterbury, South Island, New Zealand: New Zealand Geological Survey Open-File Petroleum Report 1036.

Browne, G.H., and Naish, T.R., 2003, Facies development and sequence architecture of a late Quaternary fluvial-marine transition, Canterbury Plains and shelf, New Zealand: Implications for forced regressive deposits: *Sedimentary Geology*, v. 158, p. 57–86.

Carter, R.M., 1988, Post-breakup stratigraphy of the Kaikoura synthem (Cretaceous–Cenozoic), continental margin, southeastern New Zealand: *New Zealand Journal of Geology and Geophysics*, v. 31, p. 405–429.

Carter, R.M., and Carter, L., 1982, The Motunau

fault and other structures at the southern edge of the Australian-Pacific plate boundary, offshore Marlborough, New Zealand: *Tectonophysics*, v. 88, p. 133–159.

Carter, R.M., and Gammon, P., 2004, New Zealand maritime glaciation: Millennial-scale southern climate change since 3.9 Ma: *Science*, v. 304, p. 1659–1662.

Carter, R.M., McCave, I.N., Richter, C., Carter, L., et al., 1999, Southwest Pacific gateways, Sites 1119–1125, in *Proceedings of the Ocean Drilling Program, Initial reports, Volume 181*: College Station, Texas, Ocean Drilling Program, 80 p., CD-ROM.

Carter, R.M., McCave, I.N., and Carter, L., 2004a, Fronts, flows, drifts, volcanoes, and the evolution of the southwestern gateway to the Pacific Ocean, in *Proceedings of the Ocean Drilling Program, Scientific reports, Volume 181*: College Station, Texas, Ocean Drilling Program, p. 1–111.

Carter, R.M., Gammon, P.R., and Millwood, L., 2004b, Glacial-interglacial (MIS 1–10) migrations of the Subtropical Front and paleoceanography of the Subtropical Convergence (STC) across ODP Site 1119, Canterbury Bight, southwest Pacific Ocean: *Marine Geology*, v. 205, p. 29–58.

Cooper, A.K., and O'Brien, P.E., 2004, Leg 188 Synthesis: transitions in the glacial history of the Prydz Bay region, East Antarctica, from ODP Drilling, in *Proceedings of the Ocean Drilling Program, Scientific reports, Volume 181*: College Station, Texas, Ocean Drilling Program (in press).

Cotton, C.A., 1918, Conditions of deposition on the continental shelf and slope: *Journal of Geology*, v. 26, p. 135–160.

Duplessy, J.C., Bard, E., Arnold, M., Shackleton, N.J., Duprat, J., and Labeyrie, L., 1991, How fast did the ocean-atmosphere system run during the last deglaciation?: *Earth and Planetary Science Letters*, v. 103, p. 27–40.

Faugeres, J.-C., Bonthier, E., and Stow, D.A.V., 1984, Contourite drift molded by deep Mediterranean outflow: *Geology*, v. 12, p. 296–300.

Fulthorpe, C.S., and Carter, R.M., 1991, Continental shelf progradation by sediment drift accretion: *Geological Society of America Bulletin*, v. 103, p. 300–309.

Gair, H.S., 1959, The Tertiary geology of the Pareora district, south Canterbury: *New Zealand Journal of Geology and Geophysics*, v. 2, p. 265–296.

Griffiths, G.A., and Glasby, G.P., 1985, Input of river-derived sediment to the New Zealand continental shelf: I, Mass: *Estuarine, Coastal and Shelf Science*, v. 21, p. 773–787.

Groger, M., Henrich, R., and Bickert, T., 2003, Glacial-interglacial variability in lower North Atlantic deep water: Inference from silt grain-size analysis and carbonate preservation in the western equatorial Atlantic: *Marine Geology*, v. 201, p. 321–332.

Hicks, D.M., and Shankar, U., 2003, Sediment from New Zealand rivers (chart): National Institute of Water and Atmospheric Research (NIWA) Miscellaneous Series no. 79.

Lu, H., and Fulthorpe, C.S., 2004, Controls on sequence stratigraphy of a middle Miocene–Holocene, current-swept, passive margin: Offshore Canterbury Basin, New Zealand: *Geological Society of America Bulletin* (in press).

Lu, H., Fulthorpe, C.S., and Mann, P., 2003, Three-

dimensional architecture of shelf-building sediment drifts in the offshore Canterbury Basin, New Zealand: *Marine Geology*, v. 193, p. 19–47.

Lynch-Stieglitz, J., Fairbanks, R.G., and Charles, C.D., 1994, Glacial-interglacial history of Antarctic Intermediate Water: Relative strengths of Antarctic versus Indian Ocean sources: *Paleoceanography*, v. 9, p. 7–29.

McCartney, M.S., 1982, The subtropical recirculation of mode waters: *Journal of Marine Research*, v. 40, p. 427–464.

McCave, I.N., Manighetti, B., and Beveridge, N.A.S., 1995, Circulation in the glacial North Atlantic inferred from grain-size measurements: *Nature*, v. 374, p. 149–152.

McCave, I.N., Manighetti, B., and Robinson, S.G., 1996, Sortable silt and fine sediment size/composition slicing: Parameters for palaeocurrent speed and palaeoceanography: *Paleoceanography*, v. 10, p. 593–610.

Miller, M.C., McCave, I.N., and Komar, P.D., 1977, Threshold of sediment motion under unidirectional currents: *Sedimentology*, v. 24, p. 507–528.

Morgans, H.E.G., Edwards, A.R., Scott, G.H., Graham, I.J., Kamp, P.J.J., Mumme, T.C., Wilson, G.J., and Wilson, G.S., 1999, Integrated biostratigraphy of the Waitakian-Otaian boundary stratotype, early Miocene, New Zealand: *New Zealand Journal of Geology and Geophysics*, v. 42, p. 581–614.

Morris, M., Stanton, B., and Neil, H., 2001, Subantarctic oceanography around New Zealand: Preliminary results from an ongoing survey: *New Zealand Journal of Marine and Freshwater Research*, v. 35, p. 499–519.

Norris, R.J., and Carter, R.M., 1982, Fault-bounded blocks and their role in localising sedimentation and deformation adjacent to the Alpine Fault, southern New Zealand: *Tectonophysics*, v. 87, p. 11–23.

Stanley, D.J., 1985, Mud redepositional processes as a major influence on Mediterranean margin-basin sedimentation, in Stanley, D.J., and Wenzel, F.-C., eds., *Geological evolution of the Mediterranean Basin*: New York, Springer-Verlag, p. 377–410.

Stoker, M.S., Akhurst, M.C., Howe, J.A., and Stow, D.A.V., 1998, Sediment drifts and contourites on the continental margin off northwest Britain: *Sedimentary Geology*, v. 115, p. 33–51.

Stow, D.A.V., Faugeres, J.-C., and Gonthier, E., 1986, Facies distribution and textural variation in Faro Drift contourites: Velocity fluctuation and drift growth: *Marine Geology*, v. 72, p. 71–100.

Stow, D.A.V., Faugeres, J.-C., Viana, A., and Gonthier, E., 1998, Fossil contourites: A critical review: *Sedimentary Geology*, v. 115, p. 3–31.

Sutton, P.J.H., 2003, The Southland Current: A subantarctic current: *New Zealand Journal of Marine and Freshwater Research*, v. 37, p. 645–652.

Wellman, H.W., 1971, Age of the Alpine Fault, New Zealand: *International Geological Congress*, 22nd, Delhi, India, section 4, p. 148–162.

Zachos, J., Pagani, M., Sloan, L., Thomas, E., and Billups, K., 2001, Trends, rhythms, and aberrations in global climate 65 Ma to present: *Science*, v. 292, p. 686–693.

Manuscript received 12 May 2004  
Revised manuscript received 16 July 2004  
Manuscript accepted 19 July 2004

Printed in USA

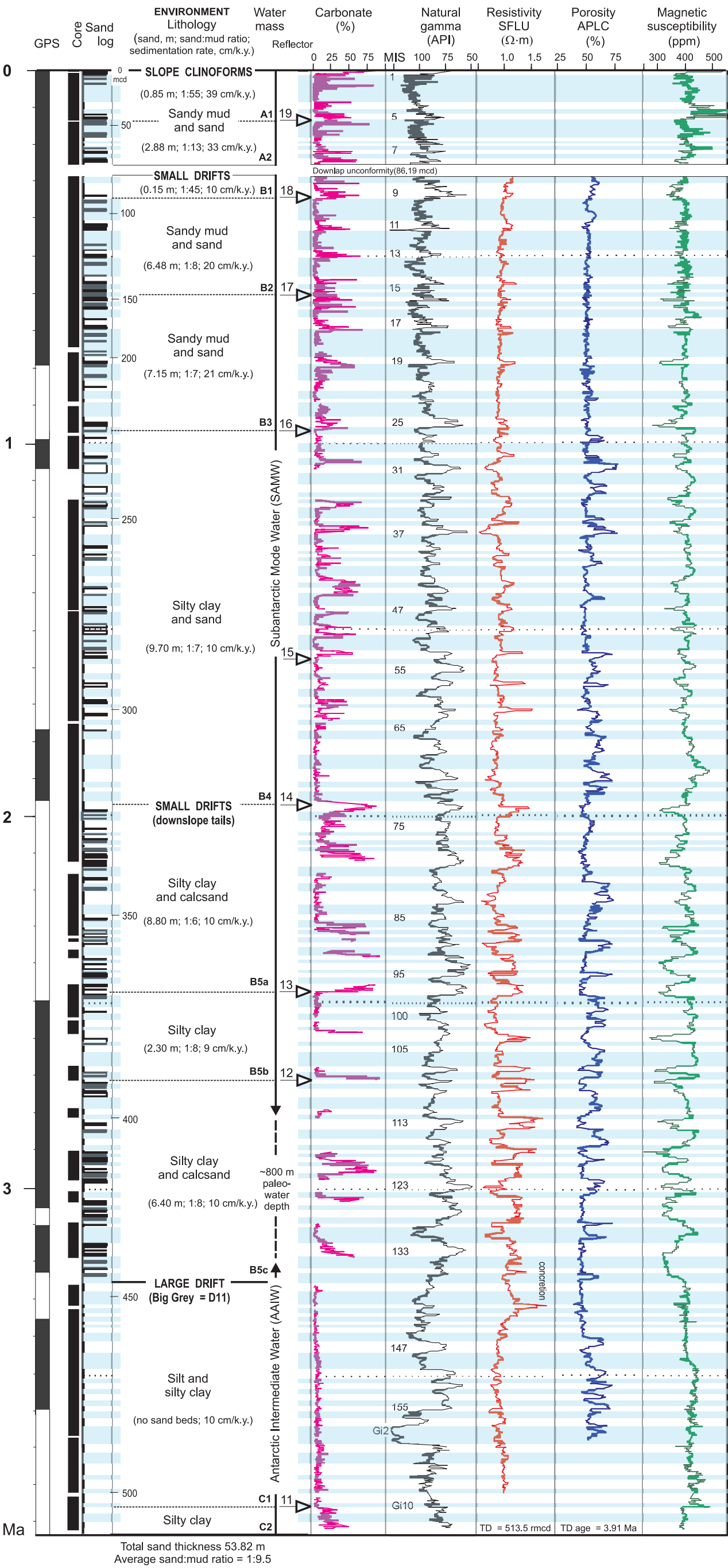


Figure 2. Lithology and physical properties for Ocean Drilling Program Site 1119 plotted against geomagnetic polarity scale (GPS) by using age model of Carter and Gammon (2004). Numbers on gamma-ray record indicate marine oxygen isotope stage (MIS). Unless otherwise indicated, all data are from Carter et al. (1999). Columns, from left: GPS; core retrieval; sand-mud log; environment and lithology; seismic sequence boundaries; carbonate percentage (based on 550 nm reflectance measurements); natural gamma-ray intensity (plotted on reversed scale to facilitate comparison with other records); resistivity (spherically focused resistivity log unaveraged, SFLU); porosity (near/array limestone porosity corrected, APLC); magnetic susceptibility. Blue overprinted horizontal lines correspond to periods of relatively cold climate, many but not all of which correspond to glacials delimited by marine oxygen isotope curves. Punctuated sand-mud stratigraphy is accompanied by rhythmic variations in clay content as reflected in natural gamma-radiation curve. Composite natural gamma-ray emission record was assembled by combining onboard multisensor track and downhole log measurements (Carter and Gammon, 2004). Signal (average resolution 1.3 k.y.) represents variations in clay content in response to waxing and waning of South Island ice cap. Controlled by these clay variations, natural gamma curve mimics closely high-resolution climatic records contained in Vostok ice core (to ca. 0.36 Ma) and deep-sea oxygen isotope curve (to ca. 3.91 Ma) (Carter and Gammon, 2004) and can therefore be used as basis for high-resolution age model for Site 1119. Sediment type is consistent across stratigraphic units A–C (cf. Fig. 1) and comprises terrigenous, micaceous, and hemipelagic mud and centimeter-bedded silt (cold climate; ~75% of total section) punctuated by intervals of mud containing normal and double-graded sand and muddy sand as thick as 1.2 m (warm climate; ~25% of total section). This stratigraphy is well reflected in petrophysical logs, in which sands are generally characterized by high carbonate content (50%–70%), low natural gamma values (50–60 API units; 90–110 API units), high resistivity (>1.2 Ω·m), and low magnetic susceptibility (300–350 ppm). Sand porosity is typically high (60%–75%), but some low-porosity sand intervals equate with either high clay content (e.g., MIS 63) or carbonate cementation (MIS ~150). Conversely, background muds are characterized by low carbonate content (1%–5%), high natural gamma values (>100 API units), low resistivity (<1.0 Ω·m), and higher magnetic susceptibility (~400 ppm). Subtle trend of increasing mean resistivity and porosity occurs across top 200 meters composite depth (mcd) (~0.9 m.y.) of section, consistent with greater percentage of sand present in upper-slope clinof orm (interval A) and topmost drift (intervals B1–B3) sediment facies.